

SEMI-AUTOMATED FOREST STAND DELINEATION USING WAVELET-BASED SEGMENTATION OF VERY HIGH RESOLUTION OPTICAL IMAGERY IN FLANDERS, BELGIUM

Frieke M.B. Van Coillie, Lieven P.C. Verbeke and Robert R. De Wulf

Laboratory of Forest Management and spatial Information Techniques
Department of Forest and Water Management, Faculty of Bio-science Engineering, Ghent University
Coupure Links 653, 9000 Ghent, Belgium
Frieke.Vancoillie@UGent.be, Lieven.Verbeke@UGent.be, Robert.Dewulf@UGent.be
<http://dfwm.ugent.be/forman>

KEY WORDS: image segmentation, forest stand delineation, wavelets

ABSTRACT:

Stand delineation estimation is one of the cornerstones of forest inventory mapping and a key element to forest management decision making. Stands are forest management units defined mainly by similar species composition, density, closure, height and age. Stand boundaries (and also attributes) are traditionally estimated through air photo interpretation. Visual interpretation is intelligibly subjective and can be remedied by numerical interpretation through automated image processing. In this paper, a stand delineation method is presented integrating wavelet analysis into the image segmentation process. It is novel in the sense that no direct spectral information is included. Using both wavelet coefficients and derived statistics, like mean absolute value and standard deviation, allowed for discrimination between forest compartments that differ in the above mentioned attributes. This approach was developed using simulated forest stands and was subsequently applied to digital aerial photographs of a forest site (representing a mixture of soft- and hardwood stands) in Flanders, Belgium. The presented method was qualitatively evaluated against traditional image segmentation i.e. segmentation based on the images' spectral information. It is concluded that the proposed method outperformed traditional image segmentation. In addition, this research was valuable to assess the added value of wavelet coefficients in object-based image segmentation.

1 INTRODUCTION

Forest stands are the basic units of management and are generally defined as spatially continuous units of uniform species composition, stem density, crown closure, height and age (Leckie et al., 2003). Correct tree species identification for example is essential for forest management and in applications such as species-specific growth models. Similarly, the calculation of timber volumes is usually species dependent. Traditionally stand boundaries have been estimated through air photo interpretation. Visual interpretation is clearly subjective and can be remedied by numerical interpretation through automated image processing (Haara and Haarala, 2002). Improved mapping techniques are constantly being sought for in terms of speed, consistency, accuracy, level of detail and overall effectiveness (Leckie et al., 2003). In this context, several techniques have been developed but most of them are designed for automated tree isolation e.g. Gougeon (1995a,b), Culvenor (2002), Larsen (1997) and Warner et al. (1998). Subsequent stand delineation based on individually outlined trees is less developed but yet fully explored by Leckie et al. (2003). They present an end-to-end process of data acquisition, tree isolation, species classification and finally stand delineation for a site representing young, dense, uniform conifer stands. One further possibility is the automatic delineation of stands based on image segmentation. Hay et al. (2005) introduced MOSS (Multi-scale Object-specific Segmentation) and showed that MOSS can be used to automatically delineate a range of objects that correspond from individual tree crowns to forest stands.

This paper presents a method aiming at forest stand delineation by wavelet-based image segmentation. In its development stage, the method uses artificially simulated images representing forest stands that differ in species composition, stem density, crown closure, height and age class. The proposed method addresses

forest stand delineation and not the extraction of other stand attributes. Next to development, the method is applied to scanned color-infrared aerial photographs with a resolution of 20cm.

2 ARTIFICIAL IMAGERY

The use of simulated remotely sensed imagery derived from artificially generated tree stands offers several advantages. First, artificially generated example stands can be large and homogeneous in terms of species composition, stem density, crown closure, height and age. Secondly, the need for validation data is alleviated since stand attributes are known in advance. Thirdly, there is total control over illumination conditions, viewing geometry and spatial resolution. Finally, the resulting images are not disturbed by atmospheric or sensor noise. As a consequence, keeping spatial resolution, illumination conditions and viewing geometry constant, errors in stand delineation are exclusively due to algorithm performance.

The generation of artificial remote sensing data is a two step process. First, a three dimensional artificial forest is generated. Afterwards this 3D model is illuminated using a ray-tracing model, and the sensor response is determined. The basic units of artificial forests or stands are artificial trees. Trees are characterized by a number of randomly distributed variables. Table 1 and Figure 1 give an overview of the random variables that control artificial tree generation. Crown projections are modelled as composed quarters of ellipses, and the crown itself is constructed by rotating an arbitrary function connecting the crown projection envelop with the tree top around the central axis of the tree.

2.1 Generation of artificial stands

Before stand generation starts, a number of artificial species is defined by choosing specific values for the parameters of the random distributions and the crown shapes shown in Table 1 and Figure 2. We used a half-ellipsoid (dilated sphere) to model a typical broadleaf species, and a semi-cone to model a typical conifer species. Additionally, it is necessary to define the allowed overlap or intersection between trees. In this study, the allowed overlap is a fixed fraction of the area of intersection between two crown projections. This parameter controls crown cover and, together with the crown radii, stand density (number of trees/ha).

Variable	Distribution	Symbol in Figure 1
stem height	normal	H_s
crown height	normal	H_c
stem diameter	normal	D_s
crown shape	half sphere / semi conical)	
crown radii	normal	d_1, d_2, d_3, d_4
stem position	uniform	(x, y)
orientation	uniform	a
spectral characteristics	normal	

Table 1: An overview of the random variables and the associated probability distributions that control artificial tree generation

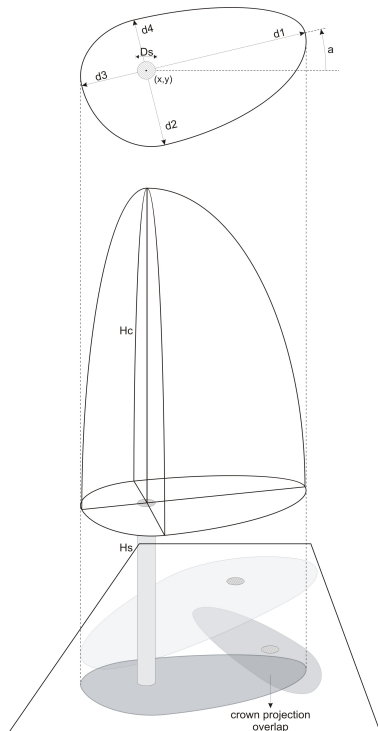


Figure 1: The applied artificial tree model

Once the artificial species are defined, a random grid is generated. Every cell in the grid is assigned a random value, corresponding to one of the generated artificial species. This grid will be used to limit the uniformly distributed positional variable of the trees. Stand/forest generation starts by randomly selecting an artificial species. A random candidate tree is then drawn from the probability distributions defined by the random species. If the position of the random tree is within one of the grid cells corresponding to the selected species, it is investigated if the candidate tree satisfies the overlap constraint by calculating the area of crown projection

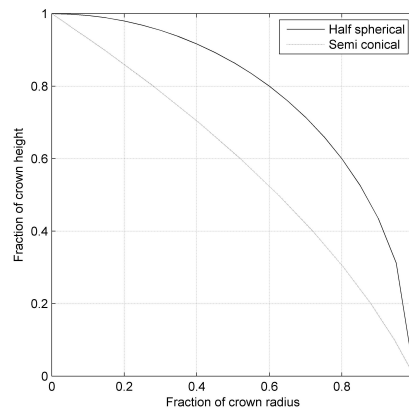


Figure 2: Crown shapes used in this work

overlap with every tree already in the forest. If no overlap constraints are violated, the tree is added to the artificial stand/forest. This process continues until a fixed number of consecutive candidate trees fails to meet the positional or overlap constraints. In order to produce artificial forests with a quasi full crown cover, it is possible to add trees of an additional, smaller species, filling up the gaps in the canopy with a kind of understorey.

2.2 Illumination of artificial stands

Once an artificial forest is generated, it needs to be converted to a simulated remotely sensed image. To do so, we used a naive ray-tracing method. The sun's position was set to its position on June 15, at 11h30 (azimuth=145°, elevation=59°) in Brussels, Belgium. The sensor's viewing angle was set to 20.5°. The image was then processed using the POV-Ray Persistence of Vision Pty. Ltd. (2004) software. The spectral characteristics are chosen in such a way that the rendered RGB images correspond to respectively the near-infrared, red and green band of an IKONOS image. Spectral characteristics were derived from in-situ measurements of *Pinus Nigra sp.*. Even though the generated scenes are assumed to contain both broadleaves and conifers, all trees were assigned the *Pinus Nigra sp.* spectral profile. This way, artificial species can only be distinguished based on structural characteristics.

3 WAVELETS

Wavelets are similar to Fourier transforms in the sense that they reconstruct/decompose signals (i.e. images) by using a superposition of translated, dilated and scaled versions of certain basis functions (Mallat, 1999). Although there exist a large number of wavelet functions, in this study wavelets from the Daubechies family (Daubechies, 2004) were used. The fast discrete wavelet transform presented by Mallat (1999) was implemented. In the algorithm, a discrete signal is decomposed in a lower scale *approximation* signal A and *detail* signal D . Extending this one-dimensional case to two dimensions (by considering rows and columns consecutively), four new images are obtained, a single approximation image and a horizontal, vertical and diagonal detail image, all at coarser scales. They applied wavelet analysis is described in more detail in Verbeke et al. (2006). For a comprehensive discourse on wavelet analysis, we advert the key publications of Daubechies (2004) and Mallat (1999).

Wavelets have been used in a variety of remote sensing applications ranging from image fusion (e.g. Park and Kang (2004);

Gonzalez-Audicana et al. (2006)), over noise and speckle reduction (e.g. Sgrenzaroli et al. (2004); Chen et al. (2006)), data compression (e.g. Zeng and Cumming (2001)), sub-pixel mapping/sharpening (e.g. Mertens et al. (2004)) to the analysis of image texture (e.g. Simard et al. (2000); Dekker (2003); Li (2004); Kandaswamy et al. (2005)). As multi-resolution wavelet analysis decomposes an image into a set of approximation and detail images at coarser scales, they are able to characterize local variability within an image at different spatial resolutions. Intuitively, stand boundaries are expected to be “highlighted” in several coarser detail images as they represent high local variability. Using this local variability, and thus statistics of wavelet coefficients such as mean absolute values and standard deviations as a basis for image segmentation, wavelet analysis is expected to allow for discrimination between forest compartments.

4 MATERIALS

The wavelet-based segmentation method was developed using artificial forest stands generated as described in Section 2. Several artificial forests were rendered with a spatial resolution of 20 cm. Both grid sizes and artificial tree species varied. Small 3x1 grids were examined, as well as large 10x10 grids. The number of artificial tree species varied, according to the grid size, from 3 to 10. Next the method was applied to color-infrared aerial photographs (scale 1:5000). Seven photographs (acquisition date: October 1987) were scanned, ortho-rectified and mosaiced yielding an image dataset with a very high spatial resolution of 20 cm. Verbeke et al. (2006) describe this process in more detail. To place the designed method into perspective, the presented method was evaluated against traditional image segmentation i.e. segmentation based on the images’ spectral information.

5 WAVELET-BASED IMAGE SEGMENTATION

Figure 3 presents a schematic overview of the applied method. The method is a segmentation procedure consisting of a segmentation and merging step.

The method starts with three-level wavelet decomposition (using the *Daubechies 4* wavelet) of the three-band input image, resulting for each spectral band in four new images (a single approximation and three detail images) at three different spatial resolution scale levels (2, 4 and 8, resp. 40, 80 and 120cm).

Based on the 27 (3 bands x 3 details x 3 scale levels) detail coefficients an image segmentation is performed. The applied segmentation algorithm is the one introduced by Baatz and Schäpe (2000), which is implemented in the eCognition software tool (eCognition, 2000). It is a bottom-up region merging technique and is therefore regarded as a region-based algorithm. The algorithm starts by considering each pixel as a separate object. Subsequently, pairs of objects are merged to form larger segments. Throughout this pairwise clustering process, the underlying optimization procedure minimizes the weighted heterogeneity nh of resulting image objects, where n is the size of a segment and h an arbitrary definition of heterogeneity. In each step, the pair of adjacent image objects which stands for the smallest growth of the defined heterogeneity is merged. If the smallest growth exceeds a user-defined threshold (the so-called scale parameter S), the process stops. The procedure simulates an even and simultaneous growth of the segments over a scene in each step and the algorithm guarantees a regular spatial distribution of the treated

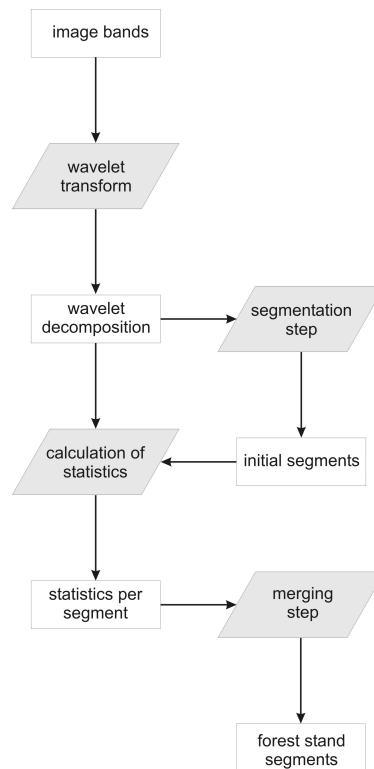


Figure 3: Schematic overview of the applied method

image objects. In this segmentation step, the algorithm utilizes spectral and shape information to extract spatially continuous, independent and homogeneous regions or image objects. The overall heterogeneity h is computed based on the spectral heterogeneity h_{color} and the shape heterogeneity h_{shape} as follows

$$f = w \cdot h_{color} + (1 - w) \cdot h_{shape} \quad (1)$$

where w is the user defined weight for color (against shape) with $0 \geq w \geq 1$.

Spectral heterogeneity is defined as

$$h_{color} = \sum_c w_c \left(n_m \cdot \sigma_c^m - (n_{obj1} \cdot \sigma_c^{obj1} + n_{obj2} \cdot \sigma_c^{obj2}) \right) \quad (2)$$

where w_c are the weights attributed to each channel and σ_c are the standard deviations of the spectral values in each channel. The standard deviations themselves are weighted by the object sizes n .

Shape heterogeneity consists of two subcriteria for smoothness and compactness

$$h_{shape} = w_{compact} \cdot h_{compact} + (1 - w_{compact}) \cdot h_{smooth} \quad (3)$$

Change in shape heterogeneity caused by a merge m is evaluated by calculating the difference between the situation after and before the merge, with

$$h_{compact} = n_m \cdot \frac{l_m}{\sqrt{n_m}} - \left(n_{obj1} \cdot \frac{l_{obj1}}{\sqrt{n_{obj1}}} + n_{obj2} \cdot \frac{l_{obj2}}{\sqrt{n_{obj2}}} \right) \quad (4)$$

and

$$h_{smooth} = n_m \cdot \frac{l_m}{b_m} - \left(n_{obj1} \cdot \frac{l_{obj1}}{b_{obj1}} + n_{obj2} \cdot \frac{l_{obj2}}{b_{obj2}} \right) \quad (5)$$

For segmentation, w is set to 0.8, $w_{compact}$ receives a value of 0.1. The scale parameter S is chosen to be rather small resulting in an over-segmentation (the ensuing segments are referred to as sub-objects). The idea is to create homogeneous objects in terms of color and shape (the latter by reduction of the deviation from a compact or smooth shape).

Next, wavelet statistics are calculated for each image sub-object: mean absolute values and standard deviations of the 27 detail coefficients are computed. This results in 54 *statistics* (i.e. images with statistical wavelet sub-object information).

Consecutively, on the basis of those statistics a merging operation is performed. In this step, sub-objects are merged into larger image objects based on the defined heterogeneity criterion. This time only *color* information is included by setting w to a value of 1. Based on the statistics derived from the wavelet detail images at three scale levels (2, 4 and 8), sub-objects are merged resulting in image segments corresponding to different forest compartments.

6 RESULTS AND DISCUSSION

Figures 4 to 8 present some details of the method results.

Figure 4 shows part of the desired result for a 10x10 grid filled up with 6 artificial tree species. In Figure 5 the result of the developed method is depicted. Wavelet-based segmentation first produces a huge amount of sub-objects that are subsequently merged, forming homogeneous objects corresponding to the desired forest compartments, as outlined by the predefined grid.

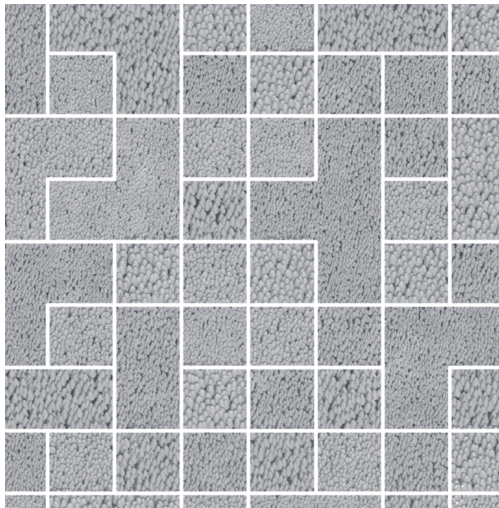


Figure 4: Part of an artificially generated forest comprising 66 stands (10x10 grid) of 6 different artificial tree species. The blue grid represents the desired stand delineation

Figure 6 shows in detail the discrimination between 4 artificial forest stands.

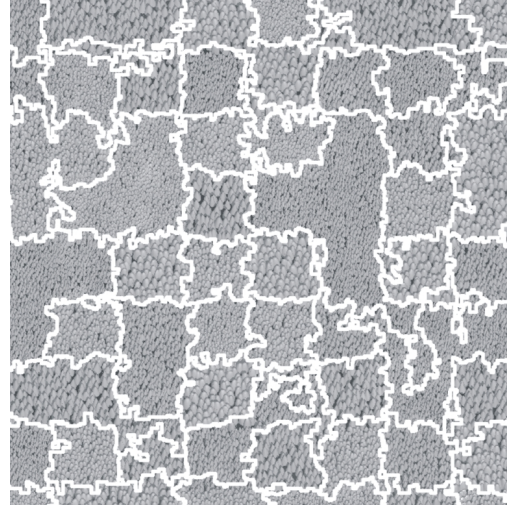


Figure 5: Wavelet-based image segmentation resulting in 64 artificial forest compartments

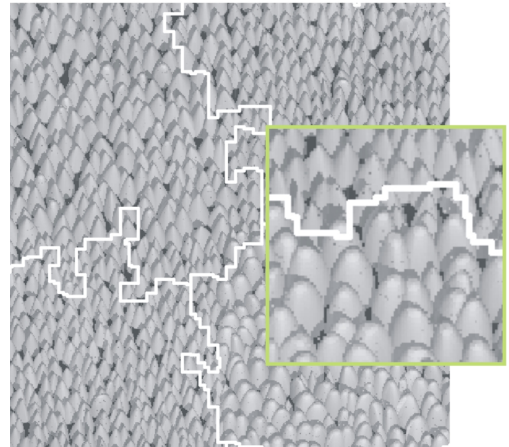
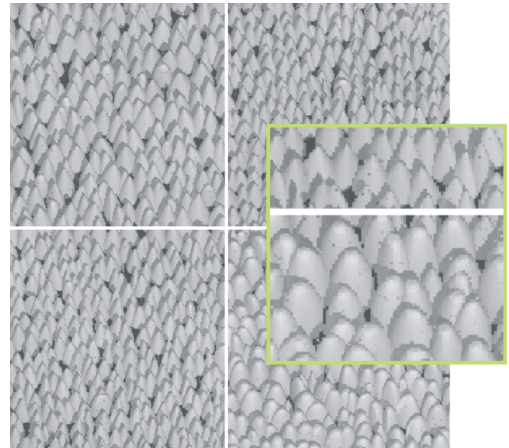


Figure 6: Detail of stand delineation. Above: expected result, below: received result

Running the segmentation process based on spectral information instead of wavelet texture, leads to poor delineation results. (Figure 7). As all artificial trees were assigned the spectral profile of *Pinus Nigra sp.*, all artificial forest stands had similar spectral characteristics and could therefore only be distinguished based on structural features. By incorporating wavelet analysis into the segmentation method, the high local variability represented by

stand boundaries is fully exploited at different spatial resolutions (wavelet scale levels). This method shows that wavelet analysis is a powerful tool to characterize local variability, which in its turn is a valuable cornerstone for image segmentation. Even when the artificial forest stands are not spectrally discernable, wavelet-based image segmentation leads to satisfactory (at least visually) stand delineation.

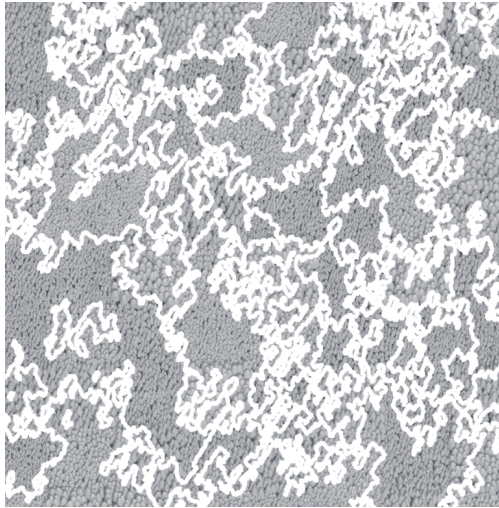


Figure 7: Segmentation based on spectral information

Next to artificial imagery, real imagery was processed. Therefore, the 20 cm color-infrared mosaic was used. No real stand boundaries were available so results could only be interpreted visually. Figures 8 to 10 provide some details. Although trees in this imagery are spectrally different, the very high spatial resolution of 20 cm induces forest stands with high (and sometimes similar) spectral heterogeneity. Spectral-based segmentation of such imagery threatens to fail and to lead to branched segments with an irregularly-shaped borderline traversing several forest compartments (Figure 10). In such cases multi-level wavelet decomposition is advantageous (Figure 9) since variability is characterized locally (as opposed to globally with Fourier transforms). Exploiting this local variability at different spatial resolutions (here at scales 2, 4, and 8, resp. 40, 80 and 160 cm) enables to distinguish between forest compartments with similar spectral characteristics but dissimilar textural properties, caused by different species composition, density, crown shape, crown closure, height and age.

7 CONCLUSIONS AND FUTURE WORK

This paper presents a new segmentation method to delineate forest compartments from very high resolution optical imagery. The method was developed using artificially generated forest stands and was applied in a later stadium to scanned color-infrared aerial photographs. The proposed method starts with multi-level wavelet decomposition. Based on the wavelet detail images (leaving out the approximation images) a segmentation is performed. For all resulting segments, wavelet derived statistics are computed. Consecutively, segments are merged on the basis of the calculated statistics. The results showed that wavelet-based image segmentation is highly advisable when forest stands are similar in terms of spectral characteristics, but different in terms of textural properties. Multi-level wavelet analysis proved to be a valuable tool to characterize local variability in image texture.



Figure 8: Detail of color-infrared mosaic, false color composite

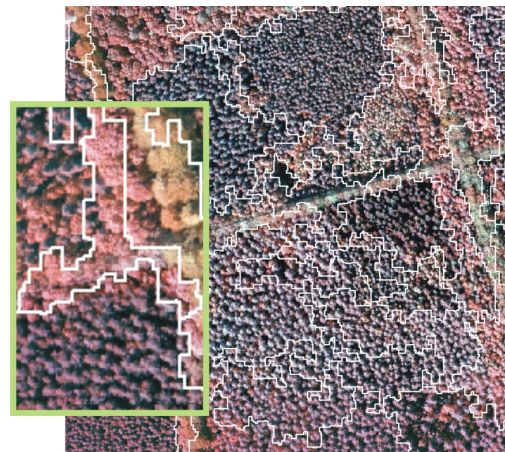


Figure 9: Wavelet-based stand delineation

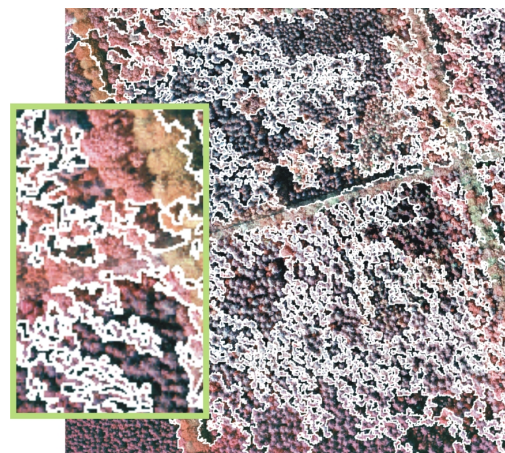


Figure 10: Segmentation based on spectral image information

The proposed method was qualitatively evaluated against spectral image segmentation. No quantitative comparison was performed. Future work will concentrate on the development of appropriate segmentation evaluation measures. Additional research will focus on the use of alternative wavelet statistics and the assessment of the most appropriate ones by applying feature selection techniques like genetic algorithms.

References

- Baatz, M. and Schäpe, A., 2000. Multiresolution segmentation - an optimization approach for high quality multi-scale image segmentation. In: J. Strobl, T. Baschke and G. Griesebner (eds), *Angewandte Geographische Informationsverarbeitung*, Wichmann-Verlag, Heidelberg, pp. 12–23.
- Chen, J. S., Lin, H., Shao, Y. and Yang, L. M., 2006. Oblique striping removal in remote sensing imagery based on wavelet transform. *INTERNATIONAL JOURNAL OF REMOTE SENSING* 27(8), pp. 1717–1723.
- Culvenor, D., 2002. Tida: an algorithm for the delineation of tree crowns in high spatial resolution remotely sensed imagery. *Computers and Geosciences* 28, pp. 33–44.
- Daubechies, I., 2004. Ten lectures on wavelets. CBMS-NSF Regional Conference Series in Applied Mathematics. Vol. 61, Society for Industrial and Applied Mathematics, Philadelphia.
- Dekker, R. J., 2003. Texture analysis and classification of ers sar images for map updating of urban areas in the netherlands. *IEEE TRANSACTIONS ON GEOSCIENCE AND REMOTE SENSING* 41(9), pp. 1950–1958.
- eCognition, 2000. Definiens imaging GmbH, Munchen, Germany.
- Gonzalez-Audicana, M., Otazu, X., Fors, O. and Alvarez-Mozos, J., 2006. A low computational-cost method to fuse ikonos images using the spectral response function of its sensors. *IEEE TRANSACTIONS ON GEOSCIENCE AND REMOTE SENSING* 44(6), pp. 1683–1691.
- Gougeon, F., 1995a. Comparison of possible multispectral classification schemes for tree crowns individually delineated on high spatial resolution MEIS images. *Canadian Journal of Remote Sensing* 21, pp. 1–9.
- Gougeon, F., 1995b. A crown-following approach to the automatic delineation of individual tree crowns in high spatial resolution aerial images. *Canadian Journal of Remote Sensing* 21, pp. 274–284.
- Haara, A. and Haarala, M., 2002. Tree species classification using semi-automatic delineation of trees on aerial images. *Scandinavian Journal of Forest Resources* 17, pp. 556–565.
- Hay, G. J., Castilla, G., Wulder, M. A. and Ruiz, J. R., 2005. An automated object-based approach for the multiscale image segmentation of forest scenes. *International Journal of Applied Earth Observation and Geoinformation* 7(4), pp. 339–359.
- Kandaswamy, U., Adjeroh, D. A. and Lee, A. C., 2005. Efficient texture analysis of sar imagery. *IEEE TRANSACTIONS ON GEOSCIENCE AND REMOTE SENSING* 43(9), pp. 2075–2083.
- Larsen, M., 1997. Crown modeling to find tree top positions in aerial photographs. In: *Proc. Third International Airborne Remote Sensing Conference and Exhibition*, Copenhagen, Denmark, Vol. II, pp. 428–435.
- Leckie, D., Gougeon, F., Walsworth, N. and Paradine, D., 2003. Stand delineation and composition estimation using semi-automated individual tree crown analysis. *Remote Sensing of Environment* 85, pp. 355–369.
- Li, J., 2004. Wavelet-based feature extraction for improved end-member abundance estimation in linear unmixing of hyperspectral signals. *IEEE TRANSACTIONS ON GEOSCIENCE AND REMOTE SENSING* 42(3), pp. 644–649.
- Mallat, S., 1999. *A wavelet tour of signal processing*. Academic Press, London.
- Mertens, K., Verbeke, L., Westra, T. and De Wulf, R., 2004. Sub-pixel mapping and sub-pixel sharpening using neural network predicted wavelet coefficients. *Remote Sensing of Environment* 91, pp. 225–236.
- Park, J. H. and Kang, M. G., 2004. Spatially adaptive multi-resolution multispectral image fusion. *INTERNATIONAL JOURNAL OF REMOTE SENSING* 25(23), pp. 5491–5508.
- Persistence of Vision Pty. Ltd., 2004. Persistence of vision (tm) raytracer. Technical report, Persistence of Vision Pty. Ltd., Williamstown, Victoria, Australia. <http://www.povray.org>.
- Sgrenzaroli, M., Baraldi, A., De Grandi, G. D., Eva, H. and Achard, F., 2004. A novel approach to the classification of regional-scale radar mosaics for tropical vegetation mapping. *IEEE TRANSACTIONS ON GEOSCIENCE AND REMOTE SENSING* 42(11), pp. 2654–2669.
- Simard, M., Saatchi, S. S. and De Grandi, G., 2000. The use of decision tree and multiscale texture for classification of jers-1 sar data over tropical forest. *IEEE TRANSACTIONS ON GEOSCIENCE AND REMOTE SENSING* 38(5), pp. 2310–2321.
- Verbeke, L. P. C., Van Coillie, F. M. B. and De Wulf, R. R., 2006. Object-based forest stand density estimation from very high resolution optical imagery using wavelet-based texture measures. In: *1st International Conference on Object-based Image Analysis (OBIA 2006)*.
- Warner, T. A., Lee, J. Y. and McGraw, J. B., 1998. Delineation and identification of individual trees in the eastern deciduous forest. In: *Proc. International Forum: Automated Interpretation of High Spatial Resolution Digital Imagery for Forestry*, Canadian Forest Service, Pacific Forestry Centre Victoria, British Columbia, p. 8191.
- Zeng, Z. H. and Cumming, I. G., 2001. Sar image data compression using a tree-structured wavelet transform. *IEEE TRANSACTIONS ON GEOSCIENCE AND REMOTE SENSING* 39(3), pp. 546–552.